www.czasopisma.pan.pl PAN POLSKA AKADEMIA NAUK www.journals.pan.pl

A R C H I V E S O F M E T A L L U R G Y A N D M A T E R I A L S

Volume 60 2015 Issue 2

DOI: 10.1515/amm-2015-0268

N. MIN*,♯, H.M. LI**, CH. XIE**, X.C. WU**

EXPERIMENTAL INVESTIGATION OF SEGREGATION OF CARBON ATOMS DUE TO SUB-ZERO CRYOGENIC TREATMENT IN COLD WORK TOOL STEEL BY MECHANICAL SPECTROSCOPY AND ATOM PROBE TOMOGRAPHY

DOŚWIADCZALNE BADANIA SEGREGACJI ATOMÓW WĘGLA W STALI NARZĘDZIOWEJ DO PRACY NA ZIMNO PO OBRÓBCE KRIOGENICZNEJ METODĄ SPEKTROSKOPII MECHANICZNEJ I TOMOGRAFII ATOMOWEJ

In this work, we present mechanical spectroscopy of cold work tool steel subjected to sub-zero cryogenic soaking treatment to reveal the carbon segregation and the subsequent carbides refinement. The maximum of Snoek-Köster (SK) peak height was obtained in the sample subjected to soaking 1h at -130°C cryogenic treatment. The SK peak height is reduced with prolonging the soaking time. The results indicate that an increase in the height of SK peak is connected with an increase in dislocation density and the number of segregated carbon atoms in the vicinity of dislocations or twin planes after martensite transformation at -130°C which is confirmed by corresponding TEM and atom probe tomography measurement. Hence, it is suggested that the isothermal martensite, formed during the cryogenic soaking treatment decreases (APT) the height of SK peak.

Keywords: Cryogenic treatment, isothermal martensite, atom probe tomography, mechanical spectroscopy, Cottrell atmosphere

W pracy przedstawiono wyniki spektroskopii mechanicznej stali narzędziowej do pracy na zimno poddanej obróbce kriogenicznej w celu odsłonięcia segregacji węgla i późniejszego tworzenia węglików. Dzięki połączeniu transmisyjnej mikroskopii elektronowej (TEM) i tomografii atomowej (APT) uzyskano maksymalny pik Snoek-Köstera (SK) w próbce poddanej obróbce kriogenicznej przez 1 godzinę w -130°C. Wysokość piku SK obniża się wraz z wydłużeniem czasu obróbki. Wyniki wskazują, że zwiększenie wysokości piku SK jest połączone ze wzrostem gęstości dyslokacji i liczby segregowanych atomów węgla w sąsiedztwie dyslokacji lub płaszczyzn bliźniaczych po przemianie martenzytycznej w -130°C, co potwierdzone jest odpowiednimi pomiarami TEM oraz APT. W związku z tym proponuje się, że izotermiczny martenzyt powstały podczas obróbki kriogenicznej zmniejsza wysokość piku SK.

1. Introduction

It is well known that the wear resistance of tool steels can be improved by cryogenic treatment due to martensitic phase transformation and nanometer sized carbides precipitated from martensite during the low temperature tempering [1]. Das *et al.* [2,3] pointed out that the effect of deep cryogenic treatment (CT) was attributed to the precipitation of fine η-carbides during tempering of martensite quenched to room temperature. It was also claimed that CT can generate decomposition of martensite by precipitation of the nanometer size carbides during tempering to room temperature. Gavriljuk *et al.* [4] pointed out that plastic deformation accompanying the low-temperature martensitic transformation in a tool steel can play a significant role in the subsequent carbide precipitation during tempering. However, the underlying mechanism of diffusion of carbon atoms and the carbide precipitation caused by cryogenic treatment has not been clarified yet. Hoyos *et al.* [5,6] studied the internal friction in martensitic carbon steels under the sub-zero temperature. The analysis of internal friction spectra indicated that mechanical loss peaks observed in the sub-zero temperature are related to the interactions between dislocations, carbon atoms and carbides. Li *et al.* [7] observed an increase in the Snoek-Köster (SK) relaxation peak after holding of the tool steel in liquid nitrogen compared with quenching at RT, and the results have been attributed to deep cryogenic treatment-increased dislocation density. Meanwhile the isothermal martensitic transformation was detected by the mechanical loss peak at around -150°C [4]. Yet it is clearly demonstrated that the evolution of microstructure and distribution of interstitial atoms in steels can be successfully detected by mechanical spectroscopy [8-11]. In this paper, the distribution of carbon atoms and structure transformation after different cryogenic treatments were studied by TEM, atom probe tomography (APT or 3-D Atom Probe) [12-15] and mechanical spectroscopy [16-18], to clarify the mechanism of carbon segregation in high alloy tool steels.

* LABORATORY FOR MICROSTRUCTURES, SHANGHAI UNIVERSITY, 99 SHANGDA ROAD, SHANGHAI, CHINA

** SCHOOL OF MATERIALS SCIENCE AND ENGINEERING, SHANGHAI UNIVERSITY, 149 YANCHANG ROAD, SHANGHAI, CHINA

♯ Corresponding author: minnacy@shu.edu.cn

2. Experimental

The material studied here is a commercial high carbon alloyed tool steel used for manufacturing products. The chemical compositions are 0.83C, 0.57Si, 9.37Cr, 0.51Mn, 1.46Mo, 0.50Ni, 0.28V (weight %). After austenitization for 10 min at 1030°C and quenching into oil, the samples were subjected to cryogenic treatment (CT), which was carried out by uniform cooling in a low-temperature cooler at -130°C for 1h, 8h, and 12h.

Conventional X-ray measurements were performed on polished samples listed in Table 1 to confirm the presence of the phases using a D/max-2200 with Cu-Kα radiation. A continuous scanning mode was chosen with the rate of 1°/min over angular with 2θ =30~ 110°. The microstructure analysis of samples was carried out in a JEOL-2010F transmission electron microscope (TEM) operated at 200kV and equipped with a high angle double-tile specimen holder.

The atom probe tomography was used as nanoscale characterization technique to analyze the distribution of carbon atoms within the investigated tool steel with 3-D atomic resolution. The sheets were cut into small rods of 0.5 mm×0.5 mm and 15 mm in length using a spark machine. Samples for APT measurements were prepared using focus ion beam milling. Needle specimens for APT analysis were prepared by standard two steps electro-polishing. Then, the needle specimens were analyzed using a CAMECA 3000 HR local electrode atom probe (LEAP). The specimens were cooled to 50 K. The pulse amplitude was kept at 20% of the standing voltage applied to the specimen. The voltage pulsing repetition rate was 200 kHz. The standing voltage on the apex of the specimen was varied automatically in order to maintain an evaporation rate of 5 ions in every 1000 pulses.

Mechanical loss measurements were carried out in a resonant internal friction apparatus (Nihon Techno Plus Co., Ltd.). The measurements of internal friction, Q^{-1}, and Young's modulus, E, were carried out in the bending mode. The samples were thin plates 1×10×55 mm^3. The resonant frequency, f_0, of the sample was in the range from 14 to 18 Hz. The internal friction was estimated from a classical method [19-22], i.e. free decaying oscillations were analyzed by an electronic discriminator recording the number of oscillations within the range of the maximum strain amplitude to the half value of this amplitude. Thus it is not surprising, that free decaying oscillations were susceptible to undesirable effects such as offset and the Zero-Point Drift (ZPD) [22]. It is assumed that such biased oscillations did not affect strongly estimated values of the internal friction. It cannot be excluded, however, offset affected high background level observed at room temperature. Young's modulus was determined from the resonant frequency, f_0, ($E \sim f^2$) using a commercial frequency meter. Mechanical loss measurements were performed in high vacuum in the temperature range from room temperature to 600°C. The heating rate used during internal friction experiments was 1.6 K/min.

3. Results and discussion

3.1. Microstructure evolution after cryogenic treatment for different soaking time

Figure 1 shows the X-ray diffraction patterns of steels after soaking at -130°C for different holding times. The volume fraction of retained austenite is calculated according to the ASTM standard E975-00, considering the diffraction crystal plane (111), (200), (220), (311) of retained austenite and (110), (200), (211), (220) of martensite. The estimated volume fraction of retained austenite is given in Table 1. The diffraction maxima of austenite are drastically decreased after CT, which indicates that the retained austenite transforms into martensite at lower temperature, and isothermal martensite at sub-zero temperature during holding times.

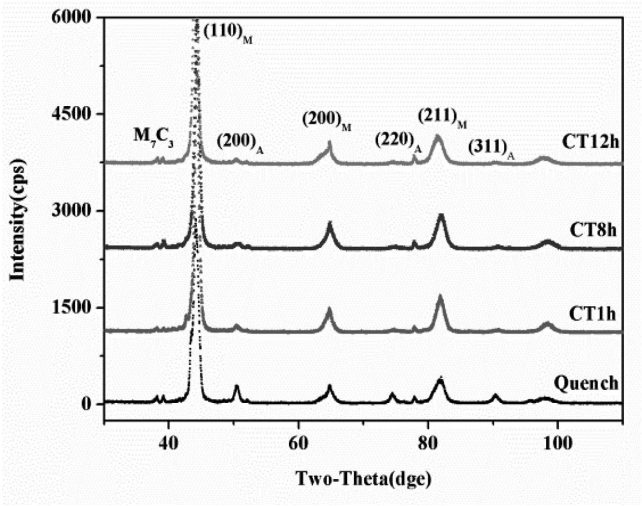

Fig. 1. X-ray diffraction patterns of the commercial high carbon alloyed tool steel after quenching and different CT soaking time at -130°C

TABLE 1

The volume fraction of retained austenite after different heat treatment

Heat treatment	Retained austenite [%]
quench	31.70
CT1h	8.13
CT8h	4.43
CT12h	3.62

CT* – cryogenic treatment

Figure 2 shows a typical TEM image of lath martensite after CT. The retained austenite is observed in between martensite laths in CT samples, which is stable after longer soaking time at -130°C. Martensitic regions contain highly twinned martensite in CT samples.

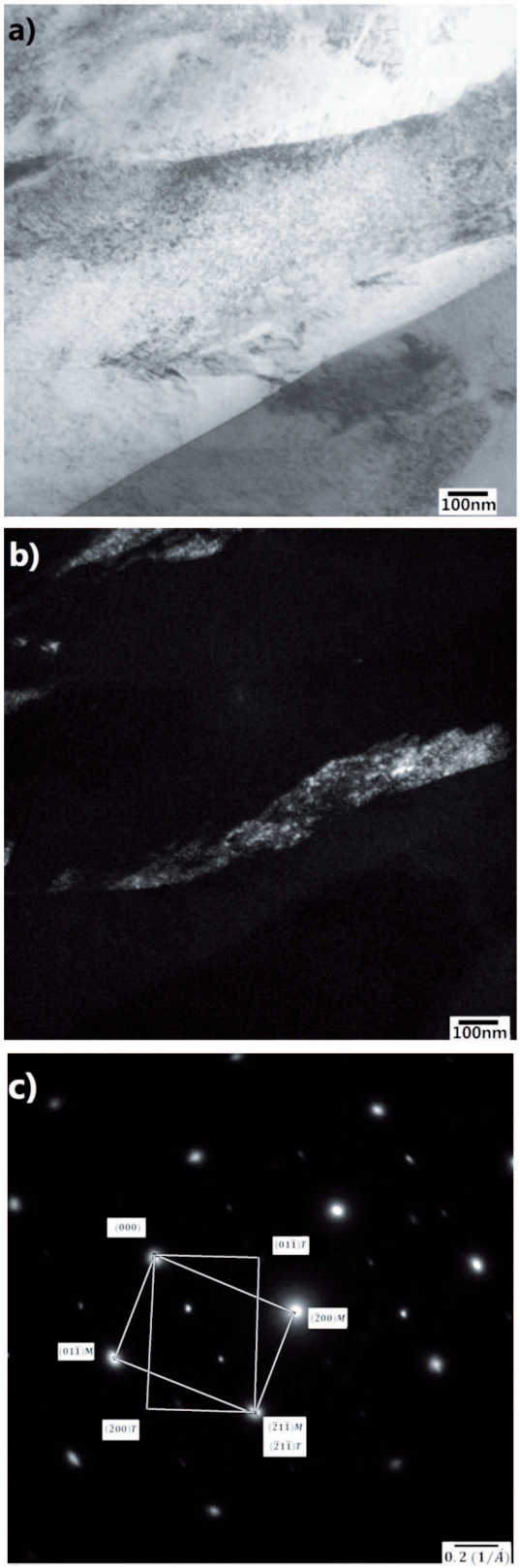

Fig. 2. Morphology and distribution of matrix with twin martensite in the CT8h sample: (a) bright field image, (b) corresponding dark field image, and (c) diffraction pattern

Figure 3(a) shows an uniform distribution map of carbon atoms measured by APT in a freshly quenched sample. The map indicates that segregation of carbon atoms is not observed. Figure 3(b) shows the distribution map of carbon atoms in the CT8h sample, that is, subjected to CT at -130°C for 8h. It is noteworthy that several carbon-enriched layers with 2-3 nm in thickness are observed in the CT8h sample. The 1-D concentration profile of carbon atoms is shown in a direction perpendicular to the carbon-enriched layers in the sample, as illustrated in Fig. 3(d). The maximum of carbon concentration inside the marked cylinder in the martensitic region is estimated as 3.92 at.%, which is higher than carbon concentration in martensite phase, but substantially lower than carbon concentration in cementite. The low-temperature induced twinning on (111) planes by martensitic transformation

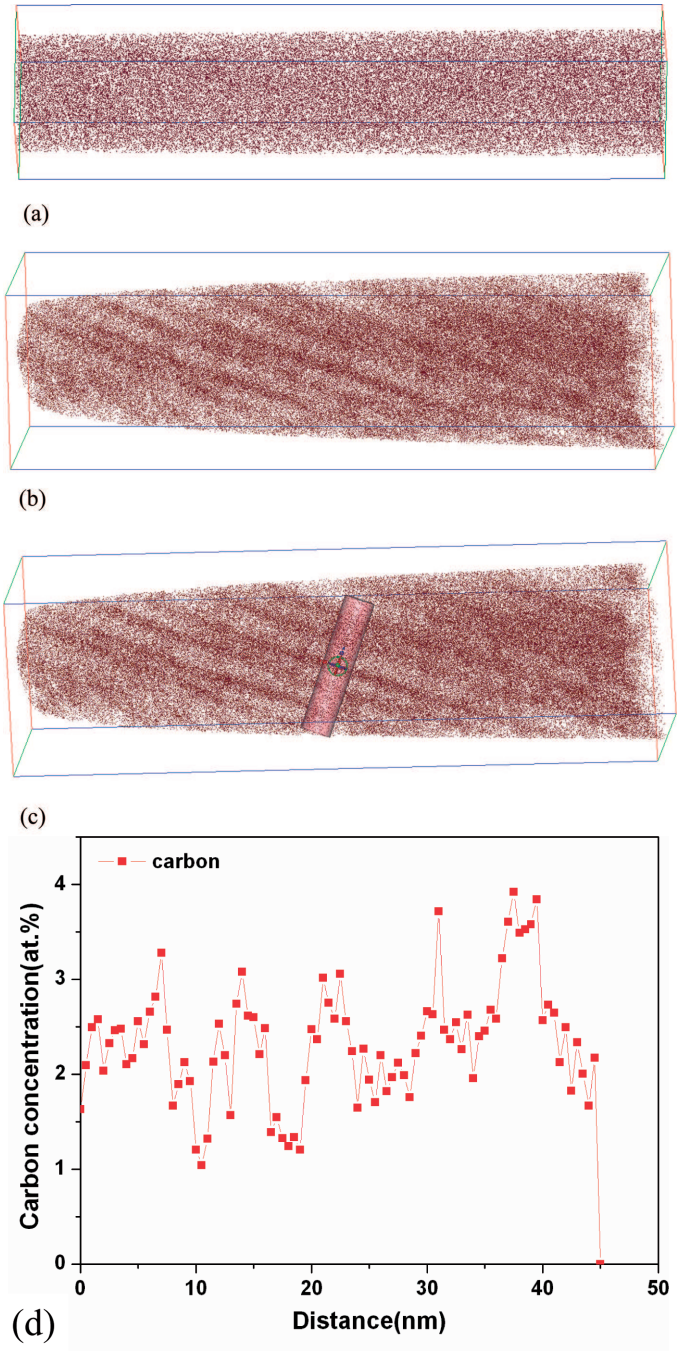

Fig. 3. (a) Carbon atom map (box size 43×42×200 nm^3) for the quenched sample. (b), (c) Carbon atom map (box size 57×56×207 nm^3) of the sample subjected to CT at -130°C for 8h. (d) 1-D carbon concentration profile in a marked cylinder of 5 nm (in diameter)×50 nm (in length) at the direction through four thin layers. (For better resolution available in colors, readers are referred to the web version of this article.)

does not affect the positions of metallic atoms but transfers the carbon atoms from the c- sub-lattice of the octahedral sites to their a- sub-lattice and b- sub-lattice [4]. Therefore, the nanometer size film layers can be regarded as the carbon segregation nearby the twin boundaries.

3.2. Snoek-Köster relaxation after quenching and cryogenic treatment

Figure 4 shows internal friction spectra and elastic modulus of SDC99 steels after quenching and CT followed by soaking at -130°C for 1h (CT1h), 8h (CT8h), and 12h (CT12h), measured in a bending pendulum. The modulus defect corresponding to SK peak is similar after quenching and soaking at -130°C. The internal friction peak shown in Fig. 4(b,c) is Snoek-Köster peak or equivalently the Snoek-Kê-Köster [23], based on the similarities of the activation energy (H = 1.5eV) obtained in measurements of SK peak in pure BCC α-Fe [24]. According to the coupling model [24-26], SK relaxation is considered as the cooperative migration of foreign interstitial atoms C, N (FIAs) which is caused by two kinds of interactions, including the FIAs themselves and between the FIAs and the strain field of dislocations [24,26,27]. Ngai *et al.* explained an increase in the activation enthalpy of SK relaxation (H^{SK}) over a wide range from 0.95eV to 2.12eV as a function of carbon concentration [24,26,27,29]. The SK peak was broader when more FIAs segregated nearby the dislocations [24,26-29]. In Fig. 4(b), it can be seen that the peak height in quenched sample is lower than that in the samples after CT. However, with prolonging soaking time, the SK peak height varies: the maximum of peak height is found in the sample after CT treated at -130°C for 1h. It is reasonable that more fractions of retained austenite transform into martensite when quenched sample is cooled down into the sub-zero temperature. Meanwhile the dislocation density increases and, thus, the height of SK peak slightly increases. The feature of this isothermal transformation is explained, the material is 'soft' due to the unaged virgin martensite [30,31] and the fraction of mobile dislocations decreases during isothermal aging, because of the formation of isothermal martensite. Therefore, the height of SK peak is reduced slightly with prolonging the soaking time at -130°C. With respect to the effect of cryogenic treatment on the microstructure evolution, the interest of many studies [2-4] was focused on the issue whether the Cottrell atmosphere at dislocations can be formed during CT treatment. The carbon atoms are essentially immobile at temperature below -100°C. Because the jumping capability of carbon atom decreases with decreasing temperature [4], carbon atoms segregated to dislocation cores (i.e., Cottrell atmosphere) or twin planes can be dragged along by dislocations. APT results indicated that carbon clusters are located nearby twin planes. Prolonged soaking treatment (at -130°C) produces the isothermal martensite and diminishes density of dislocations in the quenched martensite. Accordingly, carbon atoms segregated at twin planes with the aid of dislocations dragging effect. Thus the segregation of carbon at grain plane and decrease the dislocation density hampers the growth of carbon clusters near dislocations and subsequent carbide precipitation. Therefore, it is detrimental to abrasive wear if prolonging soaking time at -130°C.

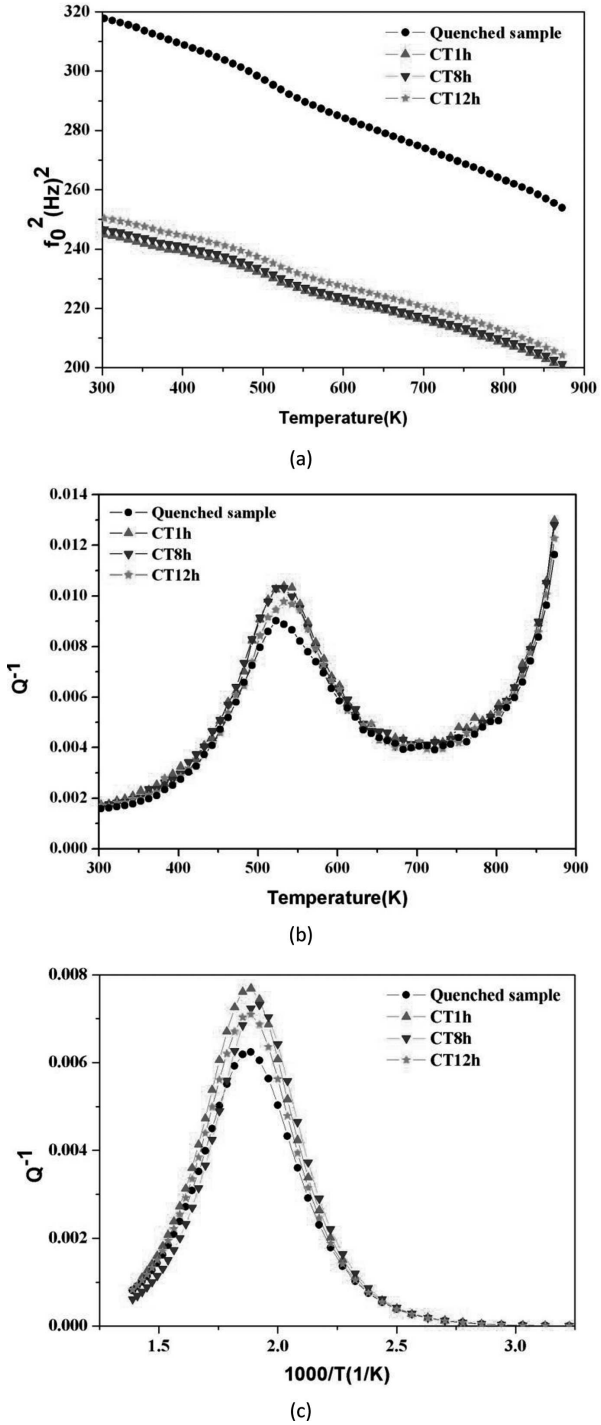

Fig. 4. Temperature variation of the relative Young's modulus ($E \sim f_o^2$) (a) and internal friction (b) in quenched sample (•) and after subsequent cryogenic treatment, CT, at -130°C for different soaking time: 1h (▲), 8h (▼), and 12h (★). (c) SK peaks in quenched samples subjected to different cryogenic treatments after subtraction of high-temperature background

4. Conclusions

The highest Snoek-Köster peak is observed in the sample subjected to cryogenic treatment at -130°C for 1h. The height of SK peak depends on the soaking time. With the aid of APT, the carbon trapping sites are identified, which indicates that carbon clusters are located nearby twin planes. These results indicate that the height of SK peak increases due to increasing

density of mobile dislocations or twin plane, and the growing amount of segregated carbon atoms after martensitic transformation at -130°C cryogenic treatment. The height of SK peak is sensitive to the amount of isothermal martensite formed during cryogenic treatment.

Acknowledgements

This work was supported by the National Natural Science Foundation of China No. 51301100 and No. 51171104.

REFERENCES

[1] P.F. Stratton, Optimising nano-carbide precipitation in tool steels, Mater. Sci. Eng. A **449-451**, 809-812 (2007).
[2] D. Das, A.K. Dutta, K.K. Ray, Influence of varied cryotreatment on the wear behavior of AISI D2 steel, Wear **266**, 297-309 (2009).
[3] D. Das, K.K Ray, On the mechanism of wear resistance enhancement of tool steels by deep cryogenic treatment, Phil. Mag. Lett. **92**, 295-303 (2012).
[4] V.G. Gavriljuk, W. Theisen, V.V. Sirosh, E.V. Polshin, A. Kortmann, G.S. Mogilny, Yu.N. Petrov, Ye.V. Tarusin, Low-temperature martensitic transformation in tool steels in relation to their deep cryogenic treatment, Acta Mater. **61**, 1705-1715 (2013).
[5] J.J. Hoyos, A.A. Ghilarducci, H.R. Salva, C.A. Chaves, J.M. Vélez, Internal friction in martensitic carbon steels, Mater. Sci. Eng. A **521-522**, 347-350 (2009).
[6] J.J. Hoyos, A.A. Ghilarducci, H.R. Salva, J. Vélez, Evolution of martensitic microstructure of carbon steel tempered at low temperatures, Proc. Mater. Sci. **1**, 185-190 (2012).
[7] S.H. Li, L.H. Deng, X.C. Wu, Y.A. Min, H.B. Wang, Influence of deep cryogenic treatment on microstructure and evaluation by internal friction of a tool steel, Cryogenics **50**, 433-437 (2010).
[8] R. Martin, D. Mari, R. Schaller, Influence of the carbon content on dislocation relaxation in martensitic steels, Mater. Sci. Eng. A **521-522**, 117-120 (2009).
[9] H. Saitoh, N. Yoshinaga, K. Ushioda, Influence of substitutional atoms on the Snoek peak of carbon in b.c.c. iron. Acta Mater. **52**, 1255-1261 (2004).
[10] I. Tkalcec, D. Mari, Internal friction in martensitic, ferritic and bainitic carbon steel cold work effects, Mater. Sci. Eng. A **370**, 213-217 (2004).
[11] R. Bagramov, D. Mari, W. Benoit, Internal friction in a martensitic high carbon steel, Phil. Mag. **81**, 2797-2808 (2001).
[12] E.A. Marquis, M. Bachhav, Y.M. Chen, Y. Dong, L.M. Gordon, A. McFarland, On the current role of atom probe tomography in materials characterization and materials science, Current Opinion in Solid State and Materials Science **17**, 217-223 (2013).
[13] F. Danoix, D. Julien, X. Sauvage, J. Copreaux, Direct evidence of cementite dissolution in drawn pearlitic steels observed by tomographic atom probe, Mater. Sci. Eng. **A 250**, 8-13 (1998).
[14] K. Hono, M. Ohnuma, M. Murayama, Cementite decomposition in heavily drawn pearlite steel wire, Scripta Mater. **977**, 44-49 (2001).
[15] E.V. Pereloma, I.B. Timokhina, J.J. Jonas, M.K. Miller, Fine-scale microstructural investigations of warm rolled low-carbon steels with and without Cr, P, and B additions, Acta Mater. **54**, 4539-4551 (2006).
[16] A.S. Nowick, B.S. Berry, Anelastic Relaxation in Crystalline Solids, Academic Press, 1972.
[17] S. Etienne, S. Elkoun, L. David, L.B. Magalas, Mechanical spectroscopy and other relaxation spectroscopies, Sol. St. Phen. **89**, 31-66 (2003).
[18] L.B. Magalas, Mechanical spectroscopy – Fundamentals, Sol. St. Phen. **89**, 1-22 (2003).
[19] L.B. Magalas, Determination of the logarithmic decrement in mechanical spectroscopy, Sol. St. Phen. **115**, 7-14 (2006).
[20] L.B. Magalas, A. Stanisławczyk, Advanced techniques for determining high and extreme high damping: OMI – A new algorithm to compute the logarithmic decrement, Key Eng. Materials **319**, 231-240 (2006).
[21] L.B. Magalas, M. Majewski, Recent advances in determination of the logarithmic decrement and the resonant frequency in low-frequency mechanical spectroscopy, Sol. St. Phen. **137**, 15-20 (2008).
[22] L.B. Magalas, M. Majewski, Ghost internal friction peaks, ghost asymmetrical peak broadening and narrowing. Misunderstandings, consequences and solution, Mater. Sci. Eng. A **521-522**, 384-388 (2009).
[23] L.B. Magalas, On the interaction of dislocations with interstitial atoms in BCC metals using mechanical spectroscopy: the Cold Work (CW) peak, the Snoek-Köster (SK) peak, and the Snoek-Kê-Köster (SKK) peak. Dedicated to the memory of Professor Ting-Sui Kê, Acta Metall. Sin. **39**, 1145-1152 (2003).
[24] L.B. Magalas, Snoek-Köster relaxation. New insights – New paradigms, J. Phys. IV **6**, 163-172 (1996).
[25] K.L. Ngai, Relaxation and Diffusion in Complex Systems, Springer, New York, 2011.
[26] K.L. Ngai, Y.N. Wang, L.B. Magalas, Theoretical basis and general applicability of the coupling model to relaxations in coupled systems, J. Alloy Comp. **211-212**, 327-332 (1994).
[27] L.B. Magalas, J.F. Dufresne, P. Moser, The Snoek-Köster relaxation in iron, J. de Phys. **42**, 127-132 (1981).
[28] Y.N. Wang, M. Gu, L. Sun, K.L. Ngai, Mechanism of Snoek-Köster relaxation in body-centered-cubic metals, Phys. Rev. B **50**, 3525-3531 (1994).
[29] L.B. Magalas, K.L. Ngai, Critical experimental data on the Snoek-Köster relaxation and their explanation by the coupling model, in Mechanics and Mechanisms of Material Damping, ASTM STP 1304, American Society for Testing and Materials, USA, 189-203 (1997).
[30] A.I. Tyshchenko, W. Theisen, A. Oppenkowski, S. Siebert, O.N. Razumova, A.P. Skoblika, V.A. Sirosha, Yu.N. Petrova, V.G. Gavriljuk, Low-temperature martensitic transformation and deep cryogenic treatment of a tool steel, Mater. Sci. Eng. A **527**, 7027-7039 (2010).
[31] G.T. Eldies, M. Cohen, Strength of initially virgin martensites at -196°C after aging and tempering, Metall. Trans. A **14**, 1007-1012 (1983).

Received: 10 March 2014.